The Eurasia Proceedings of Science, Technology, Engineering & Mathematics (EPSTEM)
ISSN: 2602-3199

The Eurasia Proceedings of Science, Technology, Engineering & Mathematics (EPSTEM), 2024

Volume 32, Pages 244-250

IConTES 2024: International Conference on Technology, Engineering and Science

Comparative Analysis of RTK and Net-RTK Accuracy in UAV-Based Photogrammetry

Oyku Alkan
Graduated Istanbul Technical University

Muntaha Kassim Alzubade
University of Technology

Mehmet Nurullah Alkan
Hitit University

Abstract: This study evaluates the positional accuracy of UAV photogrammetry using RTK and Network-based RTK (Net-RTK) methods. A two-story building was selected as the test site, and photogrammetric flights were conducted with consistent flight parameters for both RTK and Net-RTK systems. The 3D coordinates of characteristic points on the structure were digitized for both methods, with RTK-based data serving as the reference for comparison. Root Mean Square Error (RMSE) values were calculated to assess the accuracy, indicating minor random discrepancies in horizontal coordinates (Y and X) but a more notable and possible systematic error in the vertical component (H). Statistical analysis confirmed that while Y and X axis differences were random, height differences displayed a systematic trend, particularly evident in Net-RTK measurements. The results suggest that while RTK offers higher vertical accuracy suitable for precision applications, Net-RTK remains a viable alternative for general purposes, particularly in areas with reliable internet connectivity.

Keywords: GNSS, RTK, Net-RTK, UAV photogrammetry.

Introduction

The number of Unmanned Aerial Vehicles (UAVs) has significantly increased over the past decade and these devices are now actively used in a wide variety of applications. Initially developed for recreational purposes, UAVs have expanded their utility to sectors such as agriculture, mining, archaeology, construction, geology, and mapping through the acquisition and processing of digital data obtained from various mounted sensors, such as thermal cameras and LiDAR (Light Detection and Ranging). Photogrammetric flights and evaluations (Alkan et al.,2022; Alkan et al.,2023), used due to their production capabilities of 3D coordinates of objects or areas, have gained momentum due to these advancements (Vollgger & Cruden, 2016; Ozyurt & Celen, 2022; Aksoy et al., 2023; Pargiela, 2023).

Photogrammetry is defined as the science of deriving three-dimensional positional data of objects within a scene by evaluating two-dimensional images. Today, it is highly effective due to the rapid processing capabilities of digital imagery. Images derived by UAVs, with predefined forward and side overlap rates, can be analyzed through specialized software to reconstruct the region's 3D point cloud and model in digital environments. Autonomous flights with pre-set routes are typically preferred for such processes. The precision of these results varies depending on factors such as flight altitude, weather conditions, camera resolution, and type of connection to the terrestrial coordinate system. However, results with accuracies up to centimeter level are achievable. Furthermore, photogrammetric 3D digital terrain models offer numerous advantages, including rapid

point cloud production, flexible autonomous flight planning, realistic evaluation of data under actual field conditions, various outputs tailored to the objective (such as orthophotos, ortho-mosaic images, digital terrain models) (Alkan&Alzubade,2022) , repeatable measurements on the model, and the elimination of potential damage to the target object (Dering et al., 2019; Choi et al., 2023; Lenda et al., 2023; Oliveira et al., 2023; Pargiela, 2023; Specht et al., 2023; Subramanian et al., 2024, URL-1).

To create a 3D model of an area using photogrammetric methods, a typical approach involves autonomous UAV flights at low altitudes (<120 m) with forward-side overlap, capturing numerous digital images of the target. Captured images can be collectively analyzed using automated procedures like Structure-from-Motion (SfM), which enables high-accuracy 3D model generation and association with local/regional/global terrestrial coordinate systems (Woodget et al., 2017; Kenako et al., 2023; Lenda et al., 2023; Mazza et al., 2023; Pargiela, 2023, URL-2).

Scaling and positioning of a photogrammetrically produced model relative to a known terrestrial reference system is called "georeferencing." This process requires points with known coordinates, both in the model and on the actual ground. The traditional approach involves establishing Ground Control Points (GCPs) within the target area that will remain visible across all photographs. Their coordinates are measured in 3D using methods, such as GNSS observations, and then manually entered the software during digital processing. A typical model is assumed to require around 5–8 GCPs for adequate alignment with real-world coordinates, thus enabling highly accurate, centimeter-level field measurements based on the 3D model, which can save both time and cost (Vollgger & Cruden, 2016; Dering et al., 2019; Lenda et al., 2023; Pargiela et al., 2023, URL-3).

An alternative approach for georeferencing involves measuring the coordinates of photo capture points in real-time during the flight, eliminating the need for GCPs. In this case, 3D coordinate data, also known as exterior orientation parameters, are automatically calculated, facilitating high-accuracy Digital Terrain Model (DTM) production using SfM. This method can be implemented in two different ways: Real-Time Kinematic (RTK) and Network Real-Time Kinematic (Net-RTK). In the first method, a stationary GNSS station is established on a pre-observed position and transmits correction vectors in real time to the UAV. In the latter, correction vectors are obtained by connecting to a regional network via Network Transport of RTCM via Internet Protocol (NTRIP), requiring an internet connection. In both methods, the camera position at the time of capture can be determined with high accuracy during autonomous flights (Kahveci, 2017; Mazza et al., 2023; Pargiela et al., 2023; Specht et al., 2023, URL-6).

In this study, two different photogrammetric flights were conducted over a test area using both RTK and Net-RTK principles, and the characteristic points of a structure in the field were calculated for each model using a photogrammetric software. Data obtained through the RTK method were used as reference, and statistical tests were performed to examine the significance of differences with the model produced by latter. Through these analyses, the performance of the Net-RTK method in UAV-based photogrammetric field studies was evaluated.

Method

Study Area and Methodology

In this study, a building located within the campus of the Faculty of Arts and Sciences at Hitit University in Çorum was selected as the flight zone (Figure 1). This two-story building is bordered by the campus parking lot to the south and a road to the north, separated from its surroundings by a series of walls. For photogrammetric flights, the DJI Mavic 3 Enterprise was chosen. This UAV provides high resolution (20 MP) and, due to its integrated RTK unit, can connect to a local ground station or the Continuously Operating Reference Stations (CORS-TR (TUSAGA-AKTİF)) system via NTRIP. The UAV offers theoretical accuracy of 1–1.5 cm + 1 ppm both horizontally and vertically (Figure 2, URL-4).

For autonomous flights conducted with both RTK and Net-RTK, the same flight plan and altitudes (40 m) were selected to minimize potential differences between the two models during the process. Prior to the RTK-based flight, a location for the fixed station within the field was chosen, and its coordinates were determined using a CORS-TR compatible GNSS receiver by observation of 100 epochs. The UAV's remote-control device was then connected to the GNSS ground station via Wi-Fi, enabling the transmission of correction vectors. For the Net-RTK flight, the UAV's remote controller was connected to the internet through a mobile hotspot on a smartphone, and correction vectors were transmitted using the necessary login credentials for a CORS-TR account.

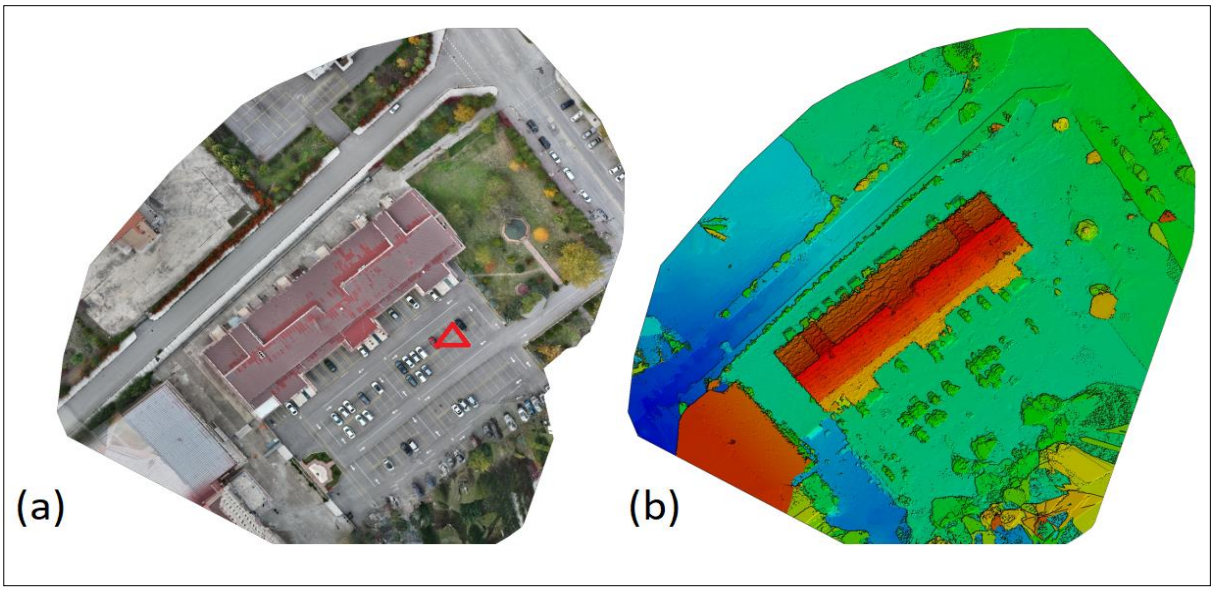

Figure 1. Study area. (a) Ortho-mosaic image, (b) Digital Terrain Model (DTM). The location of the fixed station established during the RTK-based flight is marked with a red triangle on the left (URL-5).

Figure 2. DJI Mavic 3 enterprise RTK (URL-7).
The cylindrical apparatus on top of the UAV functions as the RTK unit.

Pix4D Mapper software was chosen for photogrammetric processing in this study (URL-5). With this software, all photogrammetric images can be processed using Structure-from-Motion (SfM), generating ortho-mosaic images and point clouds via bundle block adjustment. Additionally, the software enables users to produce various outputs, such as orthophotos and DTM.

Results and Discussion

To examine the compatibility of 3D positional data, particularly for the characteristic points on the building, which are clearly observable in both models and appear in multiple digital images were selected (Figure 3). Considering the flight routes of both models, it can be stated that almost every corner of the structure, excluding the eaves, can be digitized from the model. In this study, the 3D coordinates of 10 points were compared (Figure 4). The Average Ground Sampling Distance (GSD) for both models was calculated as 1.1 cm, and the geolocation error for each of the three axes was measured to be under 0.01 m.

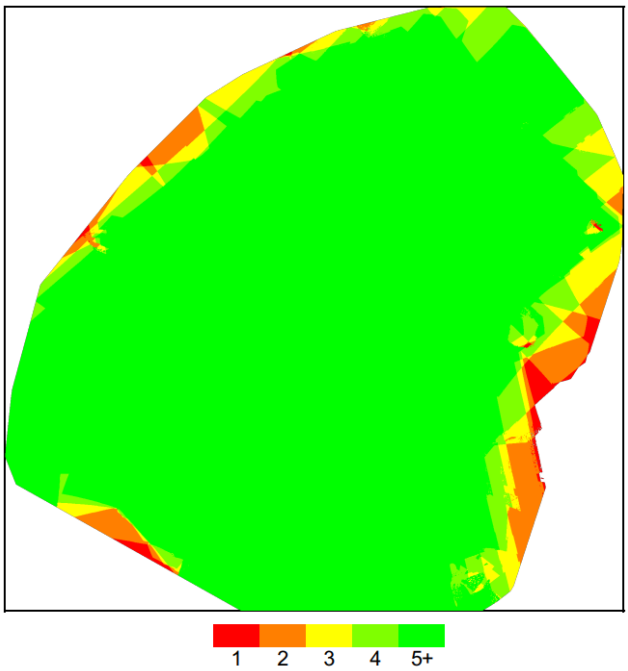

Figure 3. Number of overlapping images. Models through 1-2 images cannot be created and visualized. Main object (two-floored building) is in the green area.

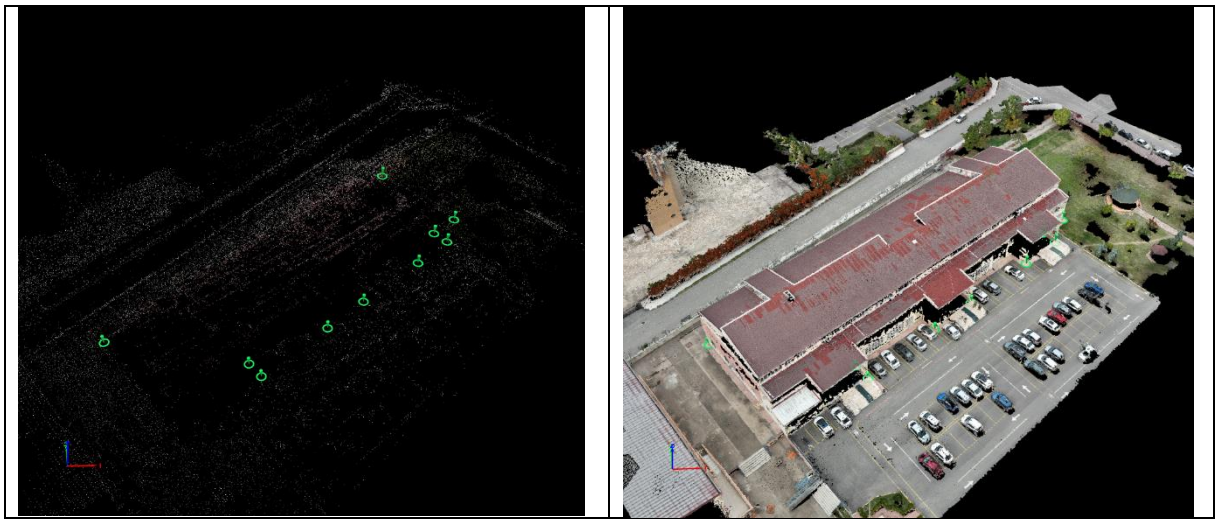

Figure 4. Selected points on the structure used for positional data comparison. On the left, building corner locations digitized through photogrammetric tie points are shown in green, while the point cloud used for digitization is displayed on the right.

Table 1. Coordinates of the characteristic points of the building.

#	Model based on RTK			Model based on NTRIP			Differences		
	Y	X	H	Y	X	H	ΔY (m)	ΔX (m)	ΔH (m)
1	409614.897	4492984.249	828.384	409614.907	4492984.244	828.308	-0.010	0.005	0.076
2	409676.809	4493036.333	828.460	409676.792	4493036.326	828.579	0.017	0.007	-0.119
3	409691.643	4493018.298	828.434	409691.629	4493018.283	828.509	0.014	0.015	-0.075
4	409685.870	4493013.479	828.495	409685.892	4493013.448	828.564	-0.022	0.031	-0.069
5	409688.286	4493010.496	828.488	409688.293	4493010.488	828.563	-0.007	0.008	-0.075
6	409680.404	4493003.783	828.528	409680.393	4493003.731	828.645	0.011	0.052	-0.117
7	409667.028	4492992.772	828.567	409667.021	4492992.782	828.687	0.007	-0.010	-0.120
8	409659.052	4492985.971	828.513	409659.032	4492985.960	828.608	0.020	0.011	-0.095
9	409645.861	4492974.808	828.528	409645.838	4492974.834	828.551	0.023	-0.026	-0.023
10	409643.509	4492977.713	828.601	409643.489	4492977.712	828.656	0.020	0.001	-0.055

Table 2. RMS and standart deviation for coordinate differences in all axes.

Metric	ΔY (m)	ΔX (m)	ΔH (m)
RMSE	0.016	0.022	0.088
Standart deviation	0.014	0.020	0.056

The point locations were initially measured using the RTK model. These 3D coordinates, considered as the reference, were then verified using the NTRIP-based model (Table 1). Root Mean Square Errors (RMSE) were also calculated for the coordinate differences in all axes (Table 2). According to Tables 1 and 2, errors in the Y and X coordinates appear to be random, while the differences in height show a systematic deviation. A graphical representation of these differences has also been provided (Figure 4).

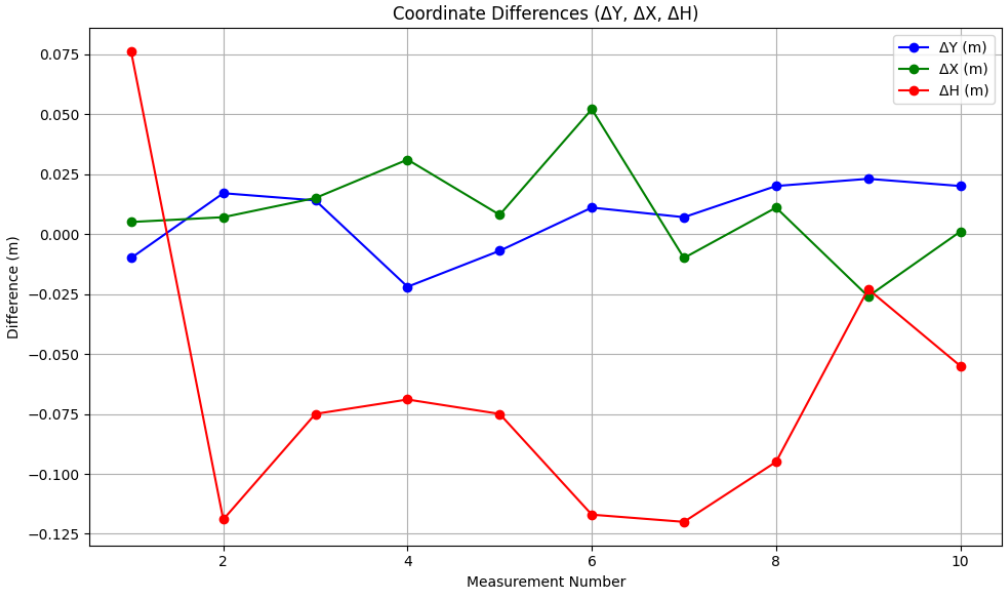

Figure 5. Coordinate differences for all axes.

In Figure 5, it can be observed that coordinate differences in the H axis almost entirely exhibit a systematic negative trend, whereas this trend appears random for the other axes. To identify this trend more clearly, statistical tests were used at this stage. In these kinds of analyses, one first should determine whether the dataset exhibits a normal distribution or not, followed by a parametric or non-parametric test to ascertain if the differences are systematic. In this study, the Shapiro-Wilk test was used to assess the distribution (Shapiro & Wilk, 1965). If the test p-value is greater than 0.05, the data is considered to fit a normal distribution for all axes (Table 3).

Table 3. Shapiro-Wilk test result for coordinate differences.

Metric	ΔY	ΔX	ΔH
Test Statistics	0.8799	0.9514	0.8190
p-value	0.1300	0.6849	0.0246
Result	Normal distribution	Normal distribution	Non-normal distribution

According to the results, the Paired t-test can be applied for coordinate differences in the Y and X axes, while the Wilcoxon, a non-parametric test, can be used for height differences (Gehan, 1965; Hedberg & Ayers, 2015). Based on these test results, it can be determined whether there is a systematic difference between the two measurement methods (Table 4). Table 4 suggests that differences in the Y and X axes are random, while height differences may contain a systematic error.

Tablo 4. Paired t-test (for ΔY and ΔX) and Wilcoxon (for ΔH) test results.

Metric	ΔY	ΔX	ΔH
Test Statistics	1.5170	1.4026	6.0000
p-value	0.1636	0.1943	0.0273
Result	Non-systematic	Non-systematic	Systematic

Conclusion

This study aimed to evaluate the positional accuracy of UAV-based photogrammetry by comparing RTK and Net-RTK methods in a controlled environment. The findings reveal that both methods yielded centimeter-level accuracies, consistent with previous research. For the coordinate differences of the 3D positional data, the horizontal coordinates (Y and X) reveal minimal random differences, with RMSE values of 0.016 m and 0.022 m, respectively. In contrast, the vertical component (H) exhibited a more significant discrepancy (RMSE = 0.088 m), suggesting a potential systematic error specific to height measurements.

Statistical analyses were used to clarify the observations. The Shapiro-Wilk test indicated that while the Y and X axes followed a normal distribution, and the H-axis data deviated from normality and requires to implement non-parametric testing. The Wilcoxon test results showed a statistically significant systematic difference in height between RTK and Net-RTK measurements ($p = 0.0273$). This aligns with recent studies that observed similar challenges in achieving consistent vertical accuracy due to the varying conditions of satellite-based correction signals in Net-RTK operations.

Results highlight the reliability of RTK for high-accuracy tasks requiring precise vertical positioning. However, for broader applications where minor vertical discrepancies are acceptable, Net-RTK remains a viable and efficient alternative, particularly in areas with robust internet connectivity. Future research could explore additional calibration techniques or hybrid methods that mitigate vertical inaccuracies in Net-RTK, especially for environments where local RTK ground stations are not feasible.

Scientific Ethics Declaration

The authors declare that the scientific ethical and legal responsibility of this article published in EPSTEM Journal belongs to the authors.

Acknowledgements or Notes

* This article was presented as an oral presentation at the International Conference on Technology, Engineering and Science (www.icontes.net) held in Antalya/Turkey on November 16-19, 2023.

References

Aksoy, B., Eylence, M., Yuksel, A.S., & Inan, S.A. (2023). Insansız hava araçları kullanılarak deforme olmuş karayolu cizgilerinin tespitinde yapay zekâ yöntemlerinin kullanılması. *Gazi Journal of Engineering Sciences*, *9*(4), 211-219.

Alkan, O., Alzubade, M.K., & Alkan, M.N. (2023) Assessing the effects of alluvial transport in the Kizilirmak river on dams with local, photogrammetric and remote sensing methods, *The Eurasia Proceedings of Science, Technology,Engineering and Mathematics, 26*, 217-224

Alkan, O., Al-Zubade, M.K., Alkan,M.N.(2022) Detection of the mineral presence and ıts effects on different tree species using drone photogrammetry and remote sensing methods, *The Eurasia Proceedings of Science, Technology,Engineering and Mathematics, 21*, 266-273.

Al-Zubade, M. K. H. & Alkan, O. (2022). The role of drone photogrammetry, remote sensing and GIS methods in the detection of ore areas and their surroundings. *The Eurasia Proceedings of Science Technology Engineering and Mathematics*, *21*, 380-387.

Choi, S. J., Lee, J. Y., Yoo, S. J., & Kim, S. H. (2023). 3D photogrammetry modeling for safety monitoring of fortress walls. *The International Archives of the Photogrammetry, Remote Sensing and Spatial Information Sciences*, *48*, 421-426.

Dering, G.M., Micklethwaite, S., Thiele, S.T., Vollgger, S.A., & Cruden, A.R. (2019). Review of drones, photogrammetry and emerging sensor technology for the study of dykes: Best practises and future potential. *Journal of Volcanology and Geothermal Research, 373*, 148–166.

Djı Enterprise. (n.d.). Mavic-3-enterprise. Retrieved from https://enterprise.dji.com/mavic-3-enterprise/specs.

Gehan, E.A. (1965). A generalized Wilcoxon test for comparing arbitrarily singly-censored samples. *Biometrika, 52*(1-2), 203–224.

Hedberg, E.C., & Ayers, S. (2015). The power of a paired t-test with a covariate. *Social Science Research, 50,* 277-291.

HKMO. (2008). *Acıklamalı örneklemeli buyuk olcekli harita ve harita bilgileri uretim yonetmenligi*. https://obs.hkmo.org.tr/show-media/resimler/ekler/7VST_ff3e350028d0cfc_ek.pdf.

Kaneko, K., Yokochi, M., Inoue, T., Kato, Y., & Fujita, H. (2023). Topographic conditions as governing factors of mire vegetation types analyzed from drone-based terrain model. *Journal of Vegetation Science, 35*(1), e13226.

Lenda, G., Borowiec, N., & Marmol, U. (2023). Study of the precise determination of pipeline geometries using uav scanning compared to terrestrial scanning, aerial scanning and uav photogrammetry. *Sensors, 23*(19), 8257.

Mazza, D., Parente, L., Cifaldi, D., Meo, A., Senatore, M.R., Guadagno, F.M., & Revellino, P. (2023). Quick bathymetry mapping of a Roman archaeological site using RTK UAS-based photogrammetry. *Frontiers in Earth Science, 11*,1183982.

Oliveira, L.L., Andriolo, A., Cremer, M.J., & Zerbini, A.N. (2023). Aerial photogrammetry techniques using drones to estimate morphometric measurements and body condition in South American small cetaceans. *Marine Mammal Science, 39*(3), 811-829.

Ozyurt, H.B., & Celen, I. H., (2022). Insansız hava araçları ile yapılan pestisit uygulamalarında farklı meme tiplerinin damla dagılımına etkisinin incelenmesi. *Tarım Makinaları Bilimi Dergisi, 18*(3), 157-172.

Pargiela, K. (2023). Optimising UAV data acquisition and processing for photogrammetry: A review. *Geomatics and Environmental Engineering, 17*(3), 29-59.

Pix4D. (n.d.). Product pix4d mapper photogrammetry software. Retrieved from https://www.pix4d.com

Pix4D. (n.d.). Retrieved from https://support.pix4d.com/hc/en-us/articles/202557489

Shapiro, S.S., & Wilk, M.B. (1965). An analysis of variance test for normality (complete samples). *Biometrika. 52*(3-4), 591-611.

SHM.(2020). *Insansız hava aracı sistemleri talimatı (SHT-IHA).* Retrieved from https://web.shgm.gov.tr/ documents/sivilhavacilik/files/mevzuat/sektorel/talimatlar.pdf

Specht, M. Widzgowski, S., Stateczny, A., Specht, C., & Lewicka, O. (2023). Comparative analysis of unmanned aerial vehicles used in photogrammetric surveys. *The International Journal on Marine Navigation and Safety of Sea Transportation, 17*(2), 433-443.

Subramanian, J.A., Asirvadam, V.S., Zulkifli, S.A.B.M., Singh, N.S.S., Shanti, N., Lagisetty, R.K., & Kadir, K.A. (2024). Integrating computer vision and photogrammetry for autonomous aerial vehicle landing in static environment. *IEEE Access*, *12*, 4532-4543.

U blox. (2024, February 1). *What is NTRIP*. Retrieved from https://www.u-blox.com/en/technologies/what-is-ntrip.

Vollgger, S.A., & Cruden, A.R. (2016). Mapping folds and fractures in basement and cover rocks using UAV photogrammetry, Cape Liptrap and Cape Paterson, Victoria, Australia. *Journal of Structural Geodesy, 85*, 168-187.

Woodget, A. S., Austrums, R., Maddock, I. P., & Habit, E. (2017). Drones and digital photogrammetry: from classifications to continuums for monitoring river habitat and hydromorphology. *Wiley Interdisciplinary Reviews: Water*, *4*(4), e1222.

Zhang, W., Peng, X., Cui, G., Wang, H., Takata, D., & Guo, W. (2023). Tree branch skeleton extraction from drone-based photogrammetric point cloud. *Drones*, *7*, 65.

Author Information

Oyku Alkan
Graduated Istanbul Technical University
İstanbul, Türkiye
Contact e-mail: *oyku*.alk*@gmail.com*

Muntaha Kassim Alzubade
University of Technology, Baghdad
Iraq

Mehmet Nurullah Alkan
Hitit University, Corum, Turkiye

To cite this article:

Alkan, O., Alzubade, M.K. & Alkan, M.N. (2024). Comparative analysis of RTK and Net-RTK accuracy in UAV-based photogrammetry. *The Eurasia Proceedings of Science, Technology, Engineering & Mathematics (EPSTEM), 32,* 244-250.